T-shaped GaAs quantum-wire lasers and the exciton Mott transition

2007 J. Phys.: Condens. Matter 19 295217

(http://iopscience.iop.org/0953-8984/19/29/295217)

IOP PUBLISHING JOURNAL OF PHYSICS: CONDENSED MATTER

J. Phys.: Condens. Matter **19** (2007) 295217 (11pp) doi:10.1088/0953-8984/19/29/295217

T-shaped GaAs quantum-wire lasers and the exciton Mott transition

M Yoshita[1,2], S M Liu[1,2], M Okano[1,2], Y Hayamizu[1,2], H Akiyama[1,2], L N Pfeiffer[3] and K W West[3]

[1] Institute for Solid State Physics (ISSP), University of Tokyo, 5-1-5 Kashiwanoha, Kashiwa, Chiba 277-8581, Japan
[2] CREST, JST, 5-1-5 Kashiwanoha, Kashiwa, Chiba 277-8581, Japan
[3] Bell Laboratories, Alcatel-Lucent, Murray Hill, NJ 07974, USA

Received 17 April 2007
Published 11 June 2007
Online at stacks.iop.org/JPhysCM/19/295217

Abstract

T-shaped GaAs quantum-wire (T-wire) lasers fabricated by the cleaved-edge overgrowth method with molecular beam epitaxy on the interface improved by a growth-interrupt high-temperature anneal are measured to study the laser device physics and fundamental many-body physics in clean one-dimensional (1D) systems. A current-injection T-wire laser that has 20 periods of T-wires in the active region and a 0.5 mm long cavity with high-reflection coatings shows a low threshold current of 0.27 mA at 30 K. The origin of the laser gain above the lasing threshold is studied with the high-quality T-wire lasers by means of optical pumping. The lasing energy is about 5 meV below the photoluminescence (PL) peak of free excitons, and is on the electron–hole (e–h) plasma PL band at a high e–h carrier density. The observed energy shift excludes the laser gain due to free excitons, and it suggests a contribution from the e–h plasma instead. A systematic micro-PL study reveals that the PL evolves with the e–h density from a sharp exciton peak, via a biexciton peak, to an e–h-plasma PL band. The data demonstrate an important role of biexcitons in the exciton Mott transition. Comparison with microscopic theories points out some problems in the picture of the exciton Mott transition.

1. Introduction

Quantum-wire lasers have been studied intensively to examine the improved device performance due to a one-dimensional (1D) density of states at the lowest energy [1–3] and also to understand the fundamental physics of electron–hole (e–h) systems in one dimension [4–7].

A quantum-wire laser was first achieved by Kapon and co-workers [8] in 1989. They fabricated GaAs V-groove wires with 9 nm × 80–100 nm sizes by metal-organic chemical vapour deposition (MOCVD), and measured continuous-wave (cw) room-temperature lasing

with about 50 mA threshold current, though lasing occurred only at higher subbands in multi-mode wires. In 1994, Tiwari and co-workers [9] fabricated quantum-wire lasers with 3-stacked InGaAs V-groove wires with 10 nm × 35 nm sizes by molecular beam epitaxy (MBE). They measured a low threshold current of 0.19 mA at room temperatures. As the current was increased, lasing was switched to higher subbands. In the same year, Wegscheider and co-workers [10] fabricated current-injection T-shaped quantum-wire (T-wire) lasers with 15 periods of GaAs T-wires with 7 nm × 7 nm sizes by a cleaved-edge overgrowth method with MBE [11]. They measured 0.4–0.7 mA threshold currents for multi-mode cw lasing in the T-wire ground states at 4 K. In 2003, Yagi and co-workers [12] fabricated 1.5 μm wavelength etching–regrowth quantum-wire lasers consisting of an 80 nm spaced array of 5-stacked 7 nm × 23 nm InGaAsP/InP rectangular wires using well-controlled systematic methods with electron-beam lithography, dry and wet etching, and MOCVD growth and regrowth. They measured room-temperature cw lasing with a threshold of 142 mA, and operating time longer than 20 000 h. In 2005, they [13] also fabricated etching–regrowth distributed-feedback quantum-wire lasers consisting of a 240 nm spaced array of 5-stacked 9 nm × 24 nm InGaAsP/InP rectangular wires. They measured cw 1.5 μm wavelength lasing with low thresholds of 2.7 mA at room temperature and 1.2 mA at 180 K.

In spite of these developments in fabrications and device characterizations, the physics of quantum-wire lasers is still not established. The device physics of quantum-wire lasers for example threshold current density per wire, transparency current density per wire, and maximum gain as a function of the injection current has not been clarified. Experimentally, these quantities have not been evaluated separately from extrinsic problems in samples. Theoretical quantitative analyses on these key characteristics beyond free-electron theories [1, 2] have not been reported.

The fundamental physics of quantum-wire lasers and quantum wires includes many problems [14–17], and has been controversial. In 1993, Wegscheider and co-workers [4] for the first time demonstrated ground-state lasing in a T-wire laser via optical pumping, and found that the lasing energy was at the peak of excitonic spontaneous emission, and was nearly independent of pump levels. This suggested the absence of band-gap renormalization and an enhanced stability of 1D excitons, so the origin of gain was ascribed to excitons. This argument induced debates on the possibilities of excitonic gain [4, 18, 19]. Furthermore, discussion on the stability of excitons at high densities and apparent absence of band-gap renormalization [20] stimulated interests in the so-called exciton Mott transition in these systems.

In this paper, we investigate the quantum-wire-laser physics and the exciton Mott transition in our high-quality GaAs T-wire lasers with improved interface smoothness by a growth-interrupt high-temperature anneal [21–24]. A current-injection T-wire laser that has 20 periods of 14 nm × 6 nm T-wires and a 0.5 mm long cavity with high-reflection coatings shows a low threshold current at 30 K of 0.27 mA, namely 0.014 mA per wire or 0.27 mA cm^{-1} per wire. The origin of the laser gain is studied with an undoped single T-wire laser by means of optical pumping. The gain is ascribed not to free excitons, or localized excitons, but to the e–h plasma at a high-density regime above the threshold. A systematic micro-photoluminescence (PL) study reveals that the PL evolves with the e–h density from a sharp exciton peak, via a biexciton peak, to an e–h-plasma PL band. The data demonstrate the important role of biexcitons in the exciton Mott transition.

2. Current-injection T-shaped quantum-wire laser

A current-injection T-wire laser [25] with 20 T-wires at the right-angle T-shaped intersections of 20 periods of 14 nm $Al_{0.07}Ga_{0.93}As$ multiple quantum wells (stem wells) and a 6 nm GaAs

quantum well (arm well) was fabricated via the cleaved-edge overgrowth method with MBE by a growth-interrupt *in situ* annealing technique [21–24]. On a (001)-oriented n^+-GaAs substrate, we successively grew an n-type GaAs buffer layer, 20 periods of 6 nm n-type GaAs/9 nm $Al_{0.35}Ga_{0.65}As$ multiple quantum wells, a 1.5 μm $(GaAs)_4(AlAs)_4$ digital-alloy lower cladding layer, 20 periods of 14 nm $Al_{0.07}Ga_{0.93}As$/44 nm $Al_{0.35}Ga_{0.65}As$ stem wells, a 1.5 μm $(GaAs)_4(AlAs)_4$ digital-alloy upper cladding layer, 100 periods of 6 nm p-type GaAs/9 nm $Al_{0.35}Ga_{0.65}As$ multiple quantum wells, and a 10 nm p-type GaAs cap layer. Si and C were used as n-type and p-type dopants, respectively, with the nominal doping level of 1×10^{18} cm^{-3}. The cleaved-edge overgrowth was then performed on its *in situ* cleaved (110) edge to form a 6 nm GaAs arm well, a 11 nm $Al_{0.5}Ga_{0.5}As$ barrier layer, a 171 nm $Al_{0.1}Ga_{0.9}As$ layer, a 1.0 μm $(GaAs)_6(AlAs)_6$ digital-alloy cladding layer, and a 10 nm GaAs cap layer.

After the MBE growth, the upper (001) layers were partially etched away so as to minimize leakage current. AuBe/Au and Ni/Ge/Au/Ni/Au were used for the p-type and n-type ohmic contacts, respectively. After evaporation of these metal films, the wafer was annealed at 450 °C for 30 min to make ohmic contacts. The p-type and n-type doped multiple-quantum-well contact layers are electrically isolated by the two undoped cladding layers and are connected only via the arm well. Under a forward bias, both electrons and holes are injected into the arm well from the n-type and p-type doped layers, and then travel to the T-wire active region via the arm well. The injection current path is thus confined in the thin arm well during laser operation.

Laser bars of cavity length of 500 μm were cut from the wafer by cleavage with the cleaved facets perpendicular to the axis of the T-wires. After deposition of a 70 nm SiO_2 insulating layer with plasma-assisted CVD, the cavity facets were high-reflection (HR) coated by a 50 nm Au layer on the front and a 300 nm one on the rear.

Figure 1 shows the light output power characteristics from the front cavity facet of the T-wire laser as a function of the bias current at 30 K, together with the output spectra at four different bias points below and above threshold. The threshold current (I_{th}) of the laser device is 0.27 mA, and the mean differential quantum efficiency η_d is 12% at 30 K. The optical spectrum is modulated by Fabry–Pérot oscillations below the threshold current and turns into a single lasing mode at 1.554 eV after the current reaches the threshold. The energy shift of lasing as the current increases to 1.5 mA is as small as 1.2 meV, showing the stability of the lasing energy from our T-wire lasers. No emission or lasing from the stem wells has been observed at all injection currents investigated, indicating high injection efficiency into the T-wires. Single-mode lasing has been similarly observed at the cryostat temperatures between 30 and 70 K.

The I_{th} of 0.27 mA at 30 K for the 20 wires corresponds to a very low current of 0.014 mA per single wire, or current density of 0.27 mA cm^{-1} per single wire. If we assume that all injected electrons and holes form e–h pairs in the wires and use a separately measured carrier lifetime of 0.4 ns, the threshold carrier density is estimated to be 7×10^5 cm^{-1} per single wire. This estimated value agrees well with our separate experimental results on optically pumped T-wire lasers. Many-body e–h states corresponding to the carrier density of 7×10^5 cm^{-1} per single wire are discussed later in this paper.

In general, one of the problems in quantum-wire lasers is a small optical confinement factor, or Γ factor, which reduces modal gain. In fact, our present T-wire laser is estimated to have small Γ factor of about 4×10^{-3}. To assist lasing with small modal gain due to small Γ factor, HR coating to the optical-cavity facets to lower mirror loss is useful. However, if the mirror loss is too low compared with internal loss, the differential quantum efficiency will be degraded. Therefore, minimization of the internal loss is important in quantum-wire lasers. In the present sample, we obtained high differential quantum efficiency η_d of 12% with HR coatings thanks to the very small internal loss α_i in the T-wire waveguide, estimated to be 0.32 cm^{-1} [25].

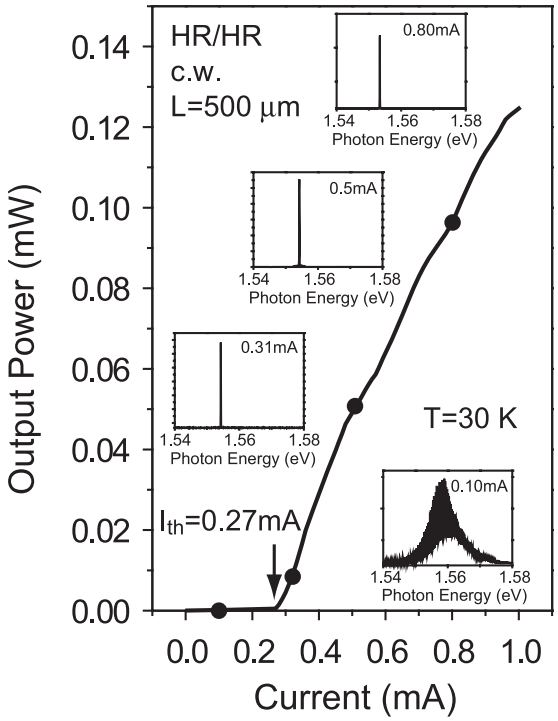

Figure 1. Light output power versus bias current characteristics and emission spectra at four different bias currents for a 20 period 14 nm × 6 nm T-wire laser diode with a 500 μm long cavity between high-reflection (HR) coated facet mirrors under cw operation at 30 K. The threshold current $I_{\rm th}$ is 0.27 mA, or 0.014 mA per single wire, and the differential quantum efficiency $\eta_{\rm d}$ is about 12% [25].

We comment finally on other current-injection T-wire-laser samples. Besides the present sample, we have studied various current-injection laser samples, which have almost the same T-wire-laser structures except for n-type and p-type doping profiles for different injection schemes [25]. They show very different temperature dependence for threshold currents, meaning that the threshold currents are rather strongly affected by transport properties in other regions than by optical properties of the wire region [26]. This suggests that basic studies on quantum-wire lasers should be made not only via current injection, but also via optical pumping [27–34], which we discuss in the next section.

3. Gain in T-shaped quantum-wire lasers

For studying the fundamental physics of quantum-wire lasers and quantum wires, undoped laser samples pumped optically are useful, because optical pumping allows versatile geometries for optical excitations and detections [27–34].

Here, we study an intrinsic single T-wire laser containing only one 14 nm × 6 nm T-wire in the active region of an undoped optical waveguide. The single T-wire laser [30] was fabricated by the cleaved-edge overgrowth method with MBE with a growth-interrupt *in situ* annealing technique [21–24], where a single wire was formed at a T-intersection of a single 14 nm (001) $Al_{0.07}Ga_{0.93}As$ stem well and a 6 nm (110) GaAs arm well. The cavity length of the lasers was 500 μm, and their cavity-mirror facets were coated by 120 nm and 300 nm thick Au films to

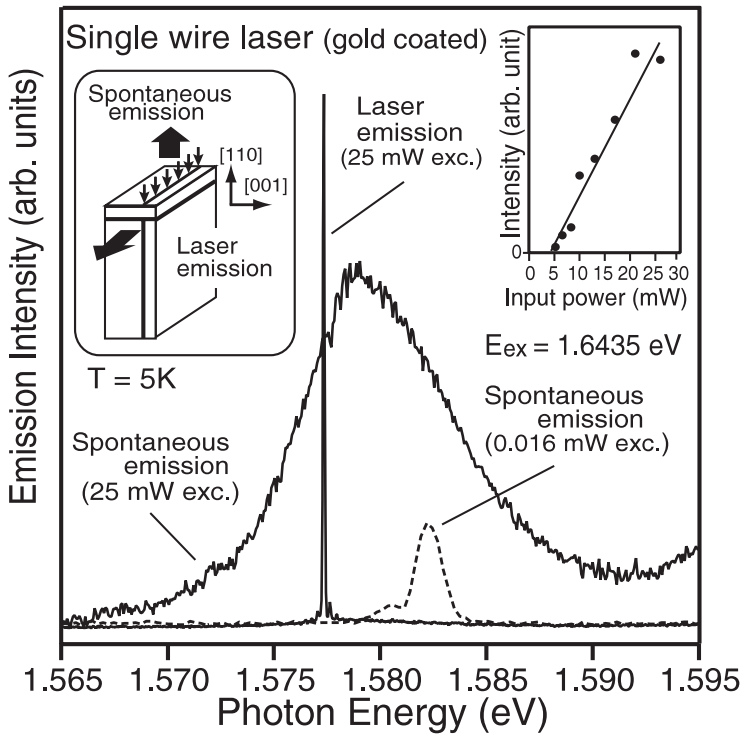

Figure 2. The solid curves show PL and laser-emission spectra of the single-wire laser with gold-coated mirrors at an excitation power of 25 mW, which is above the lasing threshold. The dashed curve shows the PL spectrum at an excitation power of 0.016 mW, which is considerably below the lasing threshold. The left inset shows a schematic diagram of the measurement setup. The right inset shows the excitation-power dependence of laser-emission intensities.

realize high reflection of about 94%. The structures and fabrication methods of the sample are described in detail in our previous reports [30].

Figure 2 shows the laser-emission and PL spectra of the single-wire laser at 5 K under optical pumping at $E_{ex} = 1.6435$ eV. The laser-emission intensities, which depend on the excitation power, indicate a threshold power of 5 mW (right inset). Solid curves show PL and laser-emission spectra of the T-wire at an excitation power of 25 mW, well above the lasing threshold. The laser emission is strongly polarized parallel to the arm well and shows single-mode lasing [30]. The dashed curve shows a PL spectrum at a very low excitation power of 0.016 mW, where the main peak at 1.582 eV and a tiny peak at a lower energy correspond to free and localized excitons, respectively [31, 33]. The lasing energy is about 5 meV below the PL peak of free excitons, and does not overlap with the peaks of free or localized excitons, which proves that lasing does not originate in free or localized excitons in the present sample. On the other hand, the PL spectrum for 25 mW excitation shows a broad PL peak which we ascribe to an e–h plasma discussed later in detail. The lasing energy is on this broad PL peak. Therefore, a gain for lasing well above the threshold was produced by the e–h plasma, though the gain mechanism near the threshold remains unsolved.

4. The exciton Mott transition in T-shaped quantum wires

Figure 3(a) shows PL spectra of a single T-wire at various excitation powers (P_{ex}) at 5 K measured by a micro-PL spectrograph method [31]. While the excitation powers are very low,

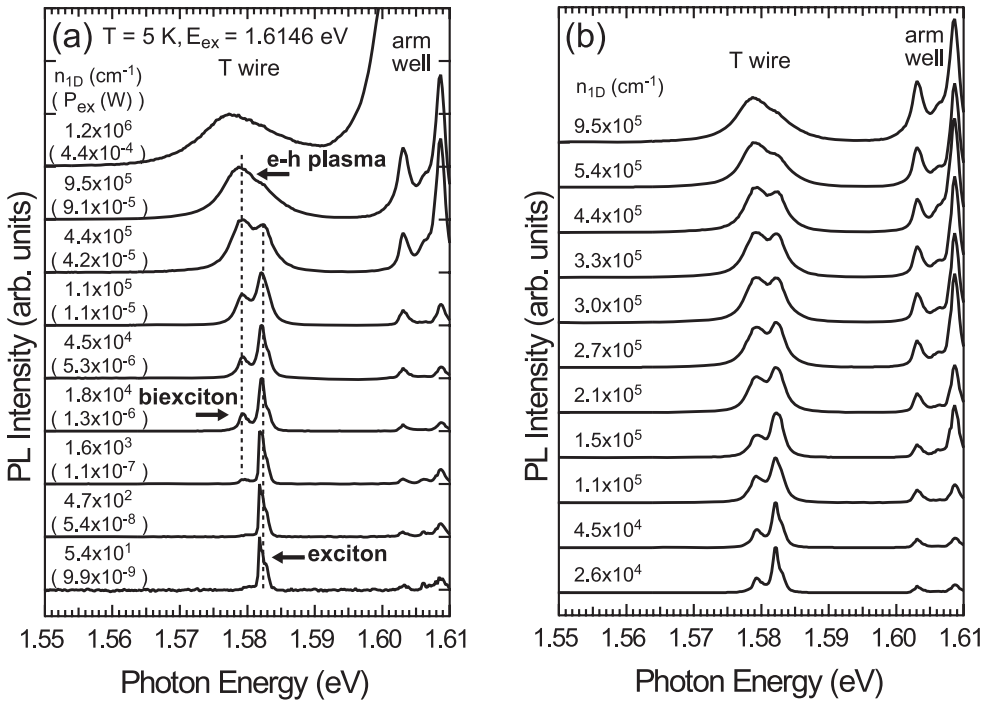

Figure 3. (a) Normalized micro-PL spectra of the single T-wire measured with the spectrograph method for various excitation powers (P_{ex}) at 5 K. Estimated 1D e–h pair densities n_{1D} are also shown. Two dashed vertical parallel lines are drawn to guide the eyes. (b) Normalized micro-PL spectra similar to (a) measured with fine steps of n_{1D} showing PL spectral change from excitons to biexcitons [31].

only a single PL peak due to 1D excitons of the wire is observed at 1.582 eV. As the excitation power is increased, a biexciton PL peak appears 2.8 meV below the exciton PL peak, and it increases its intensity superlinearly, keeping its width and its energy position. The biexciton peak overtakes the exciton peak as its width broadens, as shown more in detail in figure 3(b). Then, the biexciton PL peak changes to a broad PL peak of an e–h plasma, when the exciton PL peak fades into its high-energy tail. The PL peaks show almost no shift until this carrier density region. The plasma peak finally shows a slight red-shift and an asymmetric shape. Simultaneously, PL peaks from the arm well observed at 1.603 and 1.608 eV increase their intensities steeply.

The total PL intensity of the wire (filled squares), which is the sum of PL due to excitons and biexcitons or an e–h plasma, is plotted together with the PL intensity of the arm well (open triangles) in figure 4. The total PL intensity of the wire becomes saturated at an excitation power of about 2×10^{-4} W, while the PL intensity of the arm well still increases. This indicates that the electronic states in the wire are filled and that the Fermi filling of the arm well has started. This shows the formation of a degenerate e–h plasma in the wire, and supports the above assignment. The saturation density of e–h pairs in the wire, estimated from the 21 meV energy separation between the ground states of the wire and the arm well, is 1.2×10^6 cm^{-1}. By assuming that the PL intensity is proportional to the e–h pair density n_{1D} in the wire, we estimated n_{1D} for each PL spectrum, and show it in figure 3.

The e–h density range of superlinear increase in the biexciton PL intensity keeping its width corresponds to 4×10^3 to 1×10^5 cm^{-1}. The corresponding mean distances r_s between

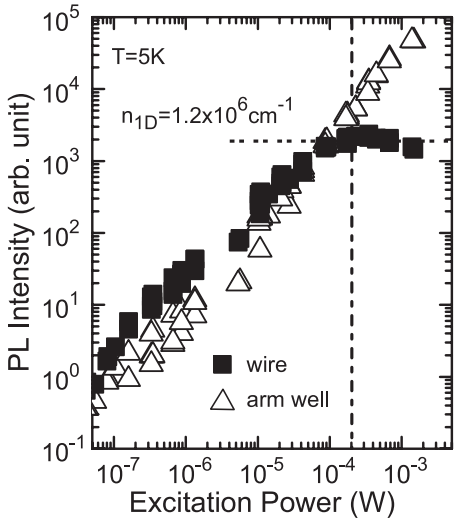

Figure 4. (a) Integrated intensities of PL from the wire (closed squares) and the arm well (open triangles) as a function of the excitation power. The PL intensity of the wire was saturated above the excitation power of 0.2 mW. The estimated saturation e–h pair density is 1.2×10^6 cm^{-1} [31].

carriers are $200a_B^*$ and $8a_B^*$, respectively, where $a_B^*(= 12.7\,\text{nm})$ is the Bohr radius of bulk GaAs. The estimated densities are reasonable values for the formation of a biexciton gas. Between 1×10^5 and 6×10^5 cm^{-1}, the width of the biexciton PL peak increases from 2 to 5 meV with the e–h density, as well as the width of the exciton PL peak. In this density region, the two PL peaks of excitons and biexcitons are well fitted by Lorentzians, which means that homogeneous broadening dominates the PL widths. These suggest increased interactions or overlaps among dense excitons and biexcitons. The e–h density when the biexciton peak overtakes the exciton peak is about 3×10^5 cm^{-1} ($r_s = 2.6a_B^*$). The e–h density when the exciton PL peak quenches is about 6×10^5 cm^{-1} ($r_s = 1.3a_B^*$). It is above 6×10^5 cm^{-1} where the PL peak of the wire is ascribed to the e–h plasma. Note that the biexciton PL changed continuously to the e–h plasma PL, and its peak position showed only small red-shift, less than 2 meV.

Figure 5 shows plots of energies and widths of the PL peaks in figure 3 as functions of the e–h pair density n_{1D} in the wire. The peak energies of excitons at 5 K are marked with filled circles, and their half-maximum widths with vertical bars. Filled diamonds show the peak energies of biexcitons or an e–h plasma at 5 K, and vertical bars show their widths. The relative size of the two symbols at each density n_{1D} approximately represents the relative intensity ratio of PL peaks. The origin and the scale of the plotted energies E is the measured onset energy E_{g0}^* of 1D continuum-state absorption and the measured energy difference E_b^* between the onset and the ground-state excitons, respectively, obtained in the low e–h density limit via PL excitation (PLE) spectra [33–35] and absorption spectra [32]. They are $E_{g0}^* = 1.593$ eV and $E_b^* = 11.4$ meV at 5 K. Since the excited exciton states due to higher Rydberg states and higher hole-subbands exist at the 1D continuum band edge [34, 35], the measured onset energy E_{g0}^* and the measured energy difference E_b^* are smaller than the expected 1D band edge $E_{g0} = 1.596$ eV and the exciton binding energy $E_b = 14$ meV, respectively, but are close to and represent them ($E_{g0}^* \sim E_{g0}$ and $E_b^* \sim E_b$). The plots clearly demonstrate the above-mentioned features observed between the e–h densities of 1×10^5 and 1×10^6 cm^{-1}, which are the constancy of PL peaks of excitons and biexcitons, the gradual switching of the exciton

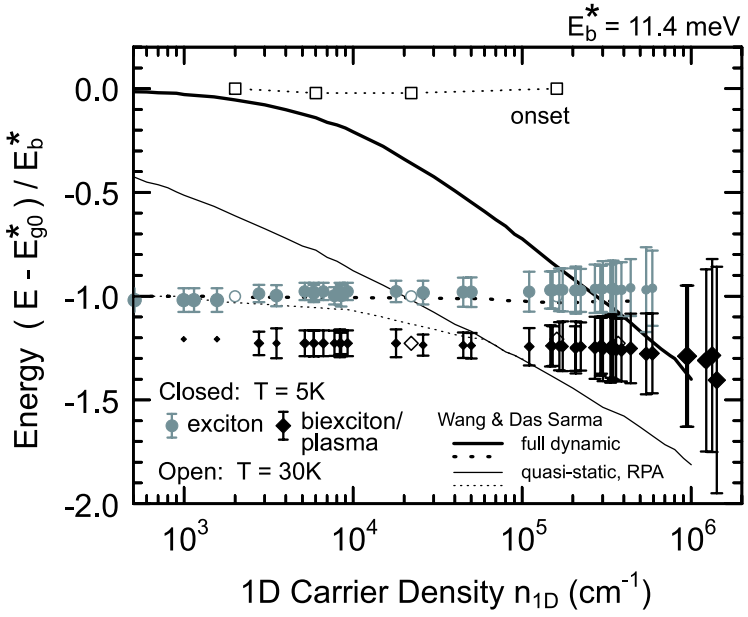

Figure 5. PL peak energies at 5 K (filled symbols) and 30 K (open symbols) for various 1D e–h carrier density n_{1D} for excitons (circles), biexcitons/e–h plasma (diamonds), and continuum band-edge onset (squares) [31]. Each vertical bar shows a half-maximum width of each PL peak. The origin and scale of the plotted energies E are the measured band-edge onset energy E^*_{g0} and the measured energy difference E^*_b between the onset and the ground-state excitons, respectively. Theoretical curves from [17] are also plotted for excitons (dashed curves) and the band edge (solid curves) calculated with dynamical (thick curves) and static (thin curves) screening functions.

PL to the biexciton PL, and the gradual change of the biexciton PL to the e–h plasma PL with broadening.

Also plotted in figure 5 by open circles, diamonds, and squares are PL energies of excitons, biexcitons/e–h plasma, and the onset of 1D continuum states, respectively, measured at 30 K. The PL energies of excitons and biexcitons/e–h plasma at 30 K are similar to those at 5 K. A difference is that PL from the onset of the 1D continuum states is observable at 30 K. Note that the onset show no shift as long as it is visible for densities up to about 2×10^5 cm^{-1}.

5. Discussions

In section 2, we estimated the threshold carrier density of 7×10^5 cm^{-1} in the current-injection T-wire laser. In section 3, we observed that the PL from the single T-wire laser emitted perpendicularly to the waveguide under optical pumping above the lasing threshold showed a broad PL peak from an e–h plasma. These results are consistent with the result that the broad PL originates from an e–h plasma for high e–h densities above 6×10^5 cm^{-1}, found in the systematic PL study in section 4. This confirms that the gain for lasing well above the threshold is produced by an e–h plasma in the quantum wire. To fully understand lasing mechanisms in quantum-wire lasers, we need to understand the data in figure 5 in relation to the exciton Mott transition.

Many theories [14–17] developing various approximation methods have been reported on the optical responses of 1D e–h systems at various densities and on the problem of the

exciton Mott transition. As shown in figure 5, we compare our experimental data with some calculated curves using dynamical (thick curves) and static (thin curves) screening functions for the ground-state exciton (dashed curves) and the band edge (solid curves) from one of the most recent papers [17]. The theoretical curves for the exciton energy, particularly the curve using the dynamical screening function, agree well with the experimental data, reproducing the very small peak shift of the wire exciton PL.

On the other hand, a significant difference is found for the band-edge shifts. Theoretical curves show very large band-edge shifts comparable to E_b for densities of 1×10^5 cm^{-1} ($r_s = 100$ nm) or 1×10^4 cm^{-1} ($r_s = 1$ μm). Experimental data have shown almost no shift of the band edge up to 2×10^5 cm^{-1}. We believe that this point is crucially important because of the following issues.

Firstly, the very small peak shift of the wire exciton PL against carrier density has often been interpreted as an exact cancellation between the shrinkage of the band gap (band-gap renormalization) and the reduction of the exciton binding energy. However, the absence of the band-edge shift up to 2×10^5 cm^{-1} demonstrates that such an explanation does not work, at least below 2×10^5 cm^{-1}.

Moreover, the exciton Mott transition is often pictured as quenching of the exciton binding energy, and hence the exciton bound states, as a result of level crossing between the rather constant exciton energy and the red-shifted renormalized band edge. However, we found that the red-shift of the band edge is absent up to 2×10^5 cm^{-1}, while broadening of PL from excitons, biexcitons, and the band edge starts near 1×10^5 cm^{-1}, and quenching of the exciton PL occurs at 6×10^5 cm^{-1}. This suggests that the prevailing picture of the exciton Mott transition is questionable.

Note that all the theories [14–17] neglected effects of biexcitons, or biexciton correlations. In experiment, the exciton–plasma crossover occurs via biexcitons. We strongly hope that a theory of the Mott transition including biexcitons is developed and compared with our experimental data.

Recently, high-density 1D e–h systems correlated through long-range Coulomb interactions were studied theoretically by using the Tomonaga–Luttinger model [36]. Therein the authors report significance of biexciton correlations in Coulomb-interacting 1D e–h systems, which was not taken into account in the previous theories. They showed that at absolute zero temperature, the system is an insulator even in the high e–h density regime, and that it has a strong instability towards biexciton crystallization. They also showed that, even at a finite temperature, the biexciton correlation dominates the other correlation effects and that the system has the character of a biexciton liquid. Hence, the 1D e–h plasma with Coulomb interactions should have strong biexciton correlations. Our experimental result that the e–h plasma emission appeared gradually at the energy position of the biexciton emission, indicating the importance of the biexciton correlations, is consistent with this theoretical result.

6. Conclusions

A current-injection T-wire laser that has 20 periods of 14 nm $\times$ 6 nm T-wires and a 0.5 mm long cavity with high-reflection coatings shows a low threshold current at 30 K of 0.27 mA, namely 0.014 mA per wire or 0.27 mA cm^{-1} per wire. The estimated threshold carrier density is 7×10^5 cm^{-1} per single wire. An optical pumping study for an undoped single T-wire laser clearly demonstrates that the gain for lasing is ascribed not to free excitons, or localized excitons, but to the e–h plasma in a high-density regime above the threshold. A systematic micro-PL study reveals that the PL evolves with the e–h density from a sharp exciton peak, via a biexciton peak, to an e–h-plasma PL band. The data demonstrate the important role

of biexcitons in the exciton Mott transition. Comparison with microscopic theories raises a question for the arguments based on the renormalized band-edge shift before the Mott transition.

Acknowledgments

We thank Professor T Ogawa, Professor K Asano, Dr P Huai, and Dr Y Tomio of Osaka University, Professor C Z Ning of NASA, and Professor H Sakaki of the University of Tokyo for valuable discussions. We acknowledge the financial support from MEXT, Japan.

References

[1] Arakawa Y and Sakaki H 1982 *Appl. Phys. Lett.* **40** 939
[2] Asada M, Miyamoto Y and Suematsu Y 1985 *Japan. J. Appl. Phys.* **24** L95
[3] Kapon E 1998 *Semiconductor Lasers I: Fundamentals* ed E Kapon (San Diego, CA: Academic) p 291
[4] Wegscheider W, Pfeiffer L N, Dignam M M, Pinczuk A, West K W, McCall S L and Hull R 1993 *Phys. Rev. Lett.* **71** 4071
[5] Ogawa T 2004 *J. Phys.: Condens. Matter* **16** S3567
Ogawa T and Takagahara T 1991 *Phys. Rev.* B **43** 14325
Ogawa T and Takagahara T 1991 *Phys. Rev.* B **44** 8138
[6] Akiyama H 1998 *J. Phys.: Condens. Matter* **10** 3095
Someya T, Akiyama H and Sakaki H 1996 *Phys. Rev. Lett.* **76** 2965
Someya T, Akiyama H and Sakaki H 1995 *Phys. Rev. Lett.* **74** 3664
Akiyama H, Someya T and Sakaki H 1996 *Phys. Rev.* B **53** R16160
[7] Akiyama H, Yoshita M, Pfeiffer L N and West K W 2004 *J. Phys.: Condens. Matter* **16** S3549
[8] Kapon E, Hwang D M and Bhat R 1989 *Phys. Rev. Lett.* **63** 430
[9] Tiwari S, Pettit G D, Milkove K R, Legoues F, Davis R J and Woodall J M 1994 *Appl. Phys. Lett.* **64** 3536
[10] Wegscheider W, Pfeiffer L, West K and Leibenguth R E 1994 *Appl. Phys. Lett.* **65** 2510
[11] Pfeiffer L N, West K W, Stormer H L, Eisenstein J P, Baldwin K W, Gershoni D and Spector J 1990 *Appl. Phys. Lett.* **56** 1697
[12] Yagi H, Sano T, Ohira K, Maruyama T, Haque A and Arai S 2003 *Japan. J. Appl. Phys.* 2 **42** L748
[13] Yagi H, Miura K, Nishimoto Y, Plumwongrot D, Ohira K, Maruyama T and Arai S 2005 *Appl. Phys. Lett.* **87** 223120
[14] Benner S and Haug H 1991 *Europhys. Lett.* **16** 579
[15] Rossi F and Molinari E 1996 *Phys. Rev. Lett.* **76** 3642
Rossi F and Molinari E 1996 *Phys. Rev.* B **53** 16462
[16] Tassone F and Piermarocchi C 1999 *Phys. Rev. Lett.* **82** 843
Piermarocchi C and Tassone F 2001 *Phys. Rev.* B **63** 245308
[17] Das Sarma S and Wang D W 2000 *Phys. Rev. Lett.* **84** 2010
Wang D W and Das Sarma S 2001 *Phys. Rev.* B **64** 195313
[18] Sirigu L, Oberli D Y, Degiorgi L, Rudra A and Kapon E 2000 *Phys. Rev.* B **61** R10575
[19] Rubio J, Pfeiffer L, Szymanska M H, Pinczuk A, He S, Baranger H U, Littlewood P B, West K W and Dennis B S 2001 *Solid State Commun.* **120** 423
[20] Ambigapathy R, Bar-Joseph I, Oberli D Y, Haacke S, Brasil M J, Reinhardt F, Kapon E and Deveaud B 1997 *Phys. Rev. Lett.* **78** 3579
[21] Yoshita M, Akiyama H, Pfeiffer L N and West K W 2001 *Japan. J. Appl. Phys.* 2 **40** L252
[22] Yoshita M, Akiyama H, Pfeiffer L N and West K W 2002 *Appl. Phys. Lett.* **81** 49
Yoshita M, Oh J W, Akiyama H, Pfeiffer L N and West K W 2003 *J. Cryst. Growth.* **251** 62
[23] Oh J W, Yoshita M, Akiyama H, Pfeiffer L N and West K W 2003 *Appl. Phys. Lett.* **82** 1709
Oh J W, Yoshita M, Hayamizu Y, Akiyama H, Pfeiffer L N and West K W 2004 *J. Appl. Phys.* **96** 6370
[24] Ishii A, Aisaka T, Oh J W, Yoshita M and Akiyama H 2003 *Appl. Phys. Lett.* **83** 4187
Ishii A, Aisaka T, Oh J W, Yoshita M, Akiyama H, Pfeiffer L N and West K W 2004 *Thin Solid Films* **464/465** 38
[25] Liu S M, Yoshita M, Okano M, Ihara T, Itoh H, Akiyama H, Pfeiffer L N, West K W and Baldwin K W 2007 *Japan. J. Appl. Phys.* 2 **46** L330
Okano M, Liu S M, Ihara T, Itoh H, Yoshita M, Akiyama H, Pfeiffer L N, West K and Malis O 2007 *Appl. Phys. Lett.* **90** 091108

[26] Kapon E, private communications
[27] Akiyama H, Pfeiffer L N, Yoshita M, Pinczuk A, Littlewood P B, West K W, Matthews M J and Wynn J 2003 *Phys. Rev.* B **67** 041302
[28] Takahashi Y, Watanabe S, Yoshita M, Itoh H, Hayamizu Y, Akiyama H, Pfeiffer L N and West K W 2003 *Appl. Phys. Lett.* **83** 4089
[29] Akiyama H, Pfeiffer L N, Pinczuk A, West K W and Yoshita M 2002 *Solid State Commun.* **122** 169
[30] Hayamizu Y, Yoshita M, Watanabe S, Akiyama H, Pfeiffer L N and West K W 2002 *Appl. Phys. Lett.* **81** 4937
[31] Yoshita M, Hayamizu Y, Akiyama H, Pfeiffer L N and West K W 2006 *Phys. Rev.* B **74** 165332
[32] Takahashi Y, Hayamizu Y, Itoh H, Yoshita M, Akiyama H, Pfeiffer L N and West K W 2005 *Appl. Phys. Lett.* **86** 243101
Takahashi Y, Hayamizu Y, Itoh H, Yoshita M, Akiyama H, Pfeiffer L N and West K W 2005 *Appl. Phys. Lett.* **87** 223119
[33] Akiyama H, Yoshita M, Pfeiffer L N, West K W and Pinczuk A 2003 *Appl. Phys. Lett.* **82** 379
[34] Itoh H, Hayamizu Y, Yoshita M, Akiyama H, Pfeiffer L N, West K W, Szymanska M H and Littlewood P B 2003 *Appl. Phys. Lett.* **83** 2043
[35] Szymanska M H, Littlewood P B and Needs R J 2001 *Phys. Rev.* B **63** 205317
[36] Asano K and Ogawa T 2005 *J. Lumin.* **112** 200